PS/AA/ACOL Note 32 28 February 1985
FC/afm

A BROADBAND SLOTLINE PICK-UP

F. Caspers

Abstract

Planar slotline and microstrip configurations on the same dielectric substrate are elements of MICs (Microwave Integrated Circuits).

It is proposed to use similar structures for pick-up or kicker applications. In this case slotlines on a metallized ceramic (Al_2O_3) substrate are positioned at a given distance from the beam with their axis transversal to the image current. The slotlines are terminated by slotline microstrip transitions, for further combination of the output signals with a microstrip combiner board.

Assuming matched transitions, only travelling waves, launched by the image current (pick-up) occur in the slotlines. It seems possible to achieve more bandwidth, higher impedance and smaller mechanical tolerances than with loop pick-ups.

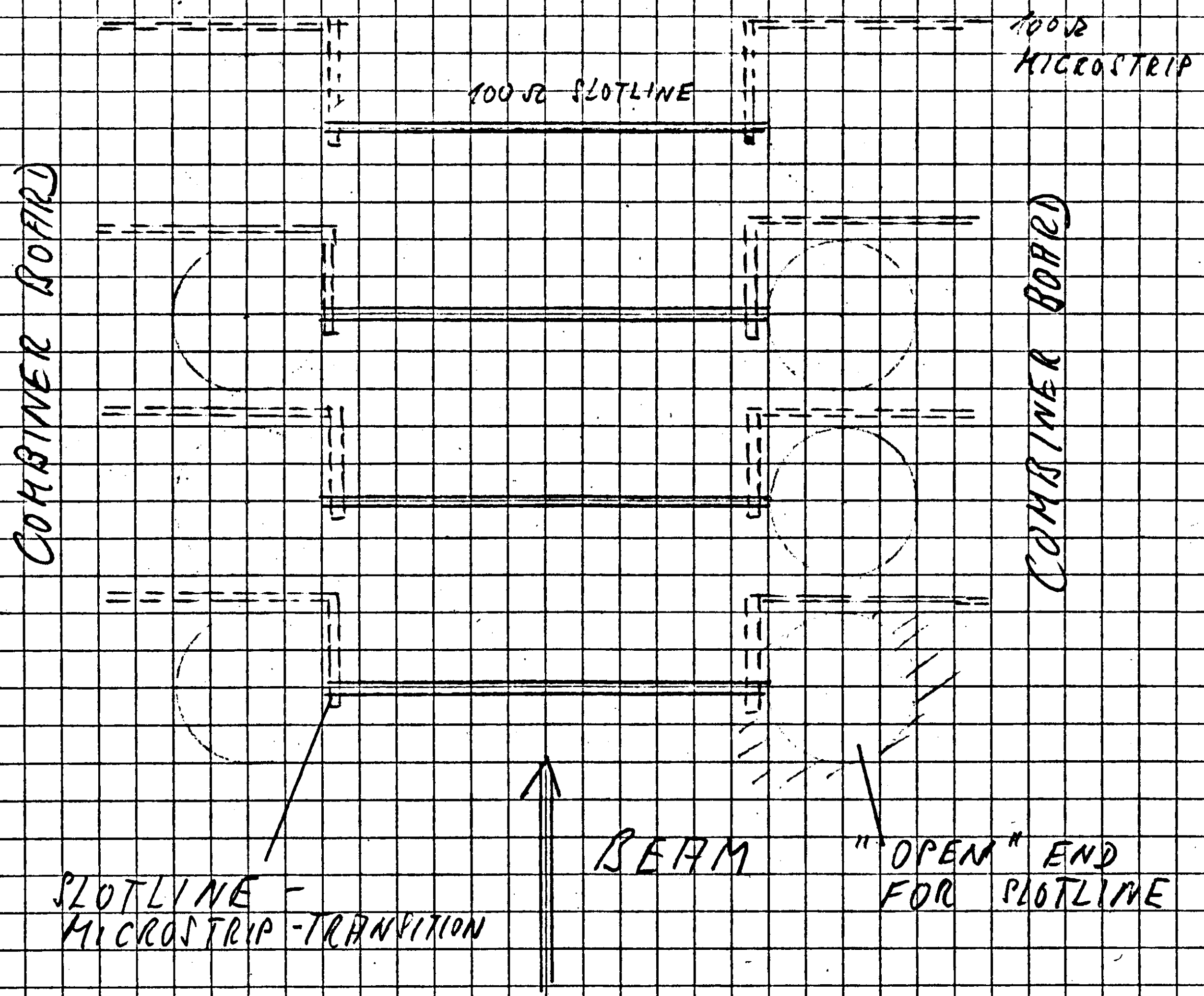
100 Ω
MICROSTRIP
100 Ω SLOTLINE
COMBINER BOARD
COMBINER BOARD
BEAM
SLOTLINE -
MICROSTRIP - TRANSITION
"OPEN" END
FOR SLOTLINE

Fig 1

2)

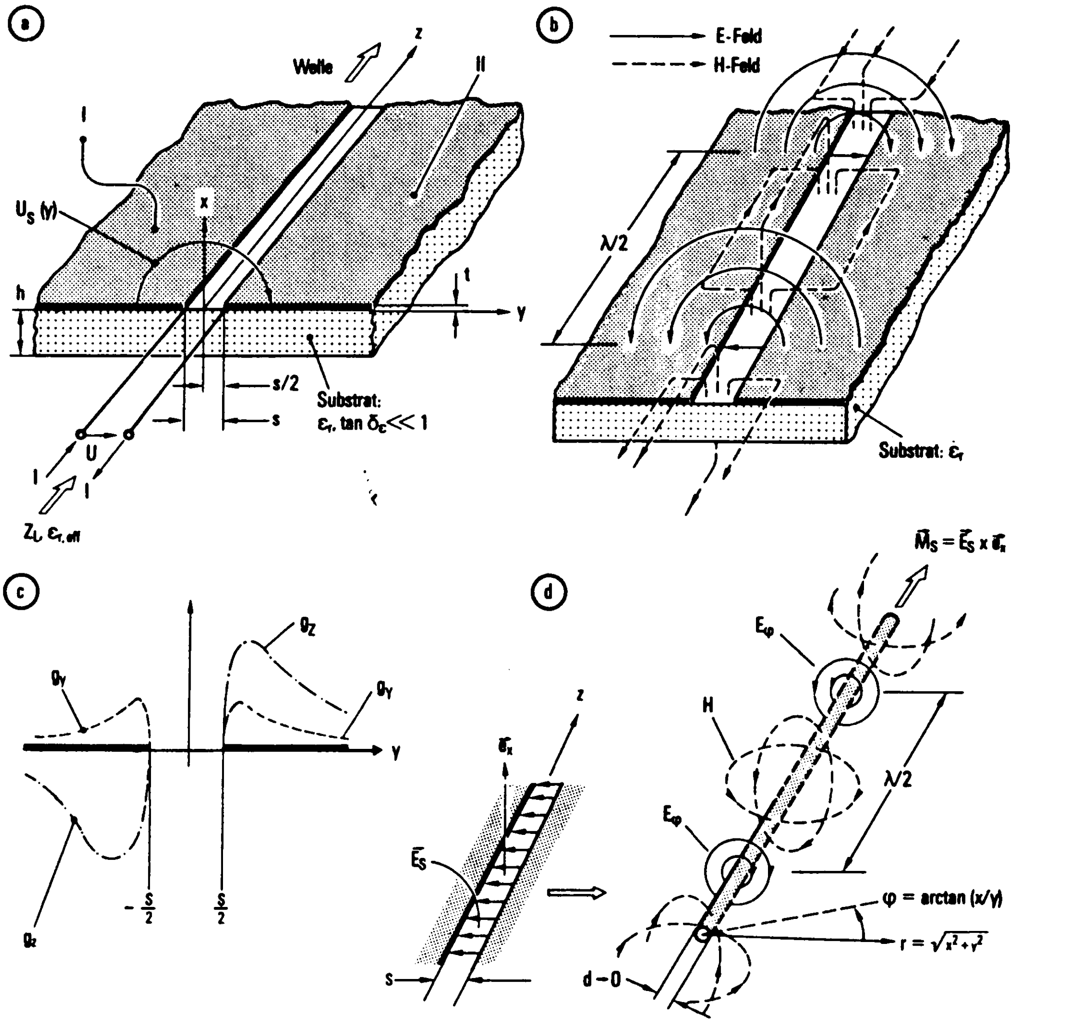

Bild 14.1. Schlitzleitung. a) Aufbau; b) Feldbild nach TE-Wellennäherung; c) qualitative Verläufe der Längs- und Querstromdichten g_z und g_y auf jeweils einer Seite der Elektroden I, II; d) magnetisches Linienstrommodell

Feldes wiederum stark frequenzabhängig ist: Mit zunehmender Frequenz konzentriert sich die Feldenergie auf eine immer enger werdende Umgebung des Schlitzes. Die Längsstromdichte g_z und Querstromdichte g_y konzentrieren sich ebenfalls in der Umgebung des Schlitzes (Bild 14.1c).

Fig 1a: SLOTLINE-FIELDS

[2]

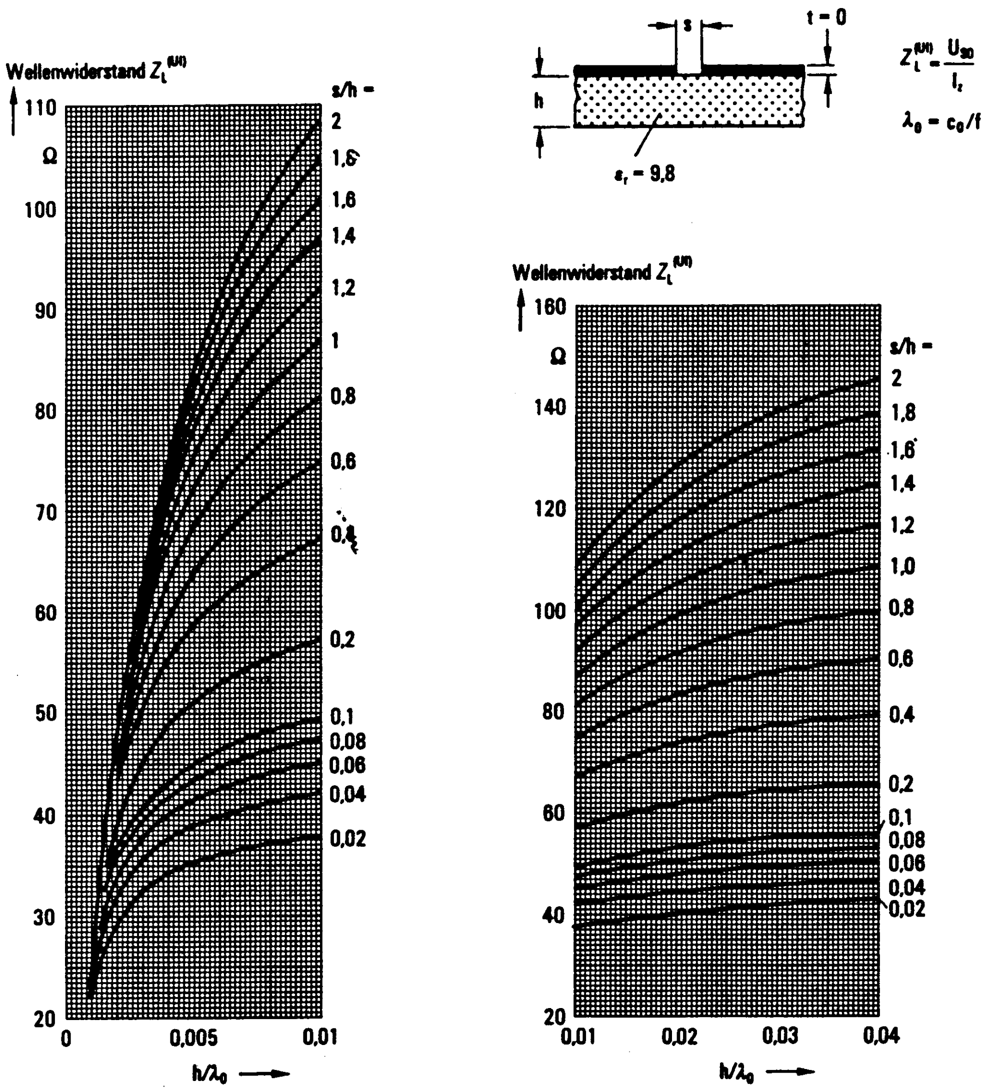

Bild 14.4. Wellenwiderstand $Z_L^{(UI)}$ der Schlitzleitung auf Al_2O_3-Keramiksubstrat ($\varepsilon_r = 9{,}8$) nach der Spannungs-Strom-Definition, berechnet nach der Variationsmethode /14.3/.

Fig 2 SLOTLINE-IMPEDANCE [2]

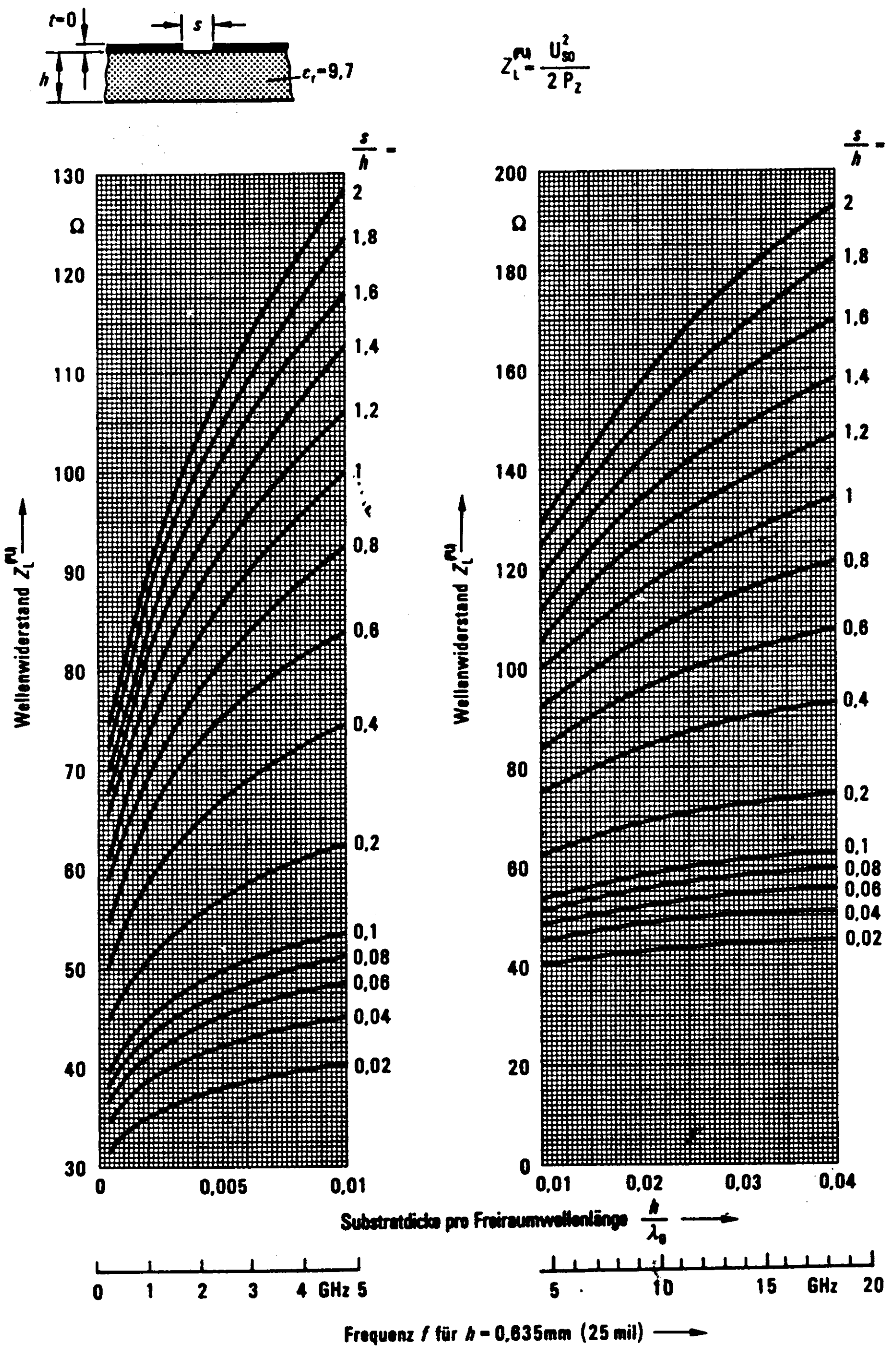

Bild 14.2. Wellenwiderstand $Z_L^{(PU)}$ der Schlitzleitung auf Al_2O_3-Keramiksubstrat ($\varepsilon_r = 9{,}7$) nach der Spannungs-Leistungsdefinition, berechnet nach dem Hohlleiterblendenmodell / 1.349/.

(4)

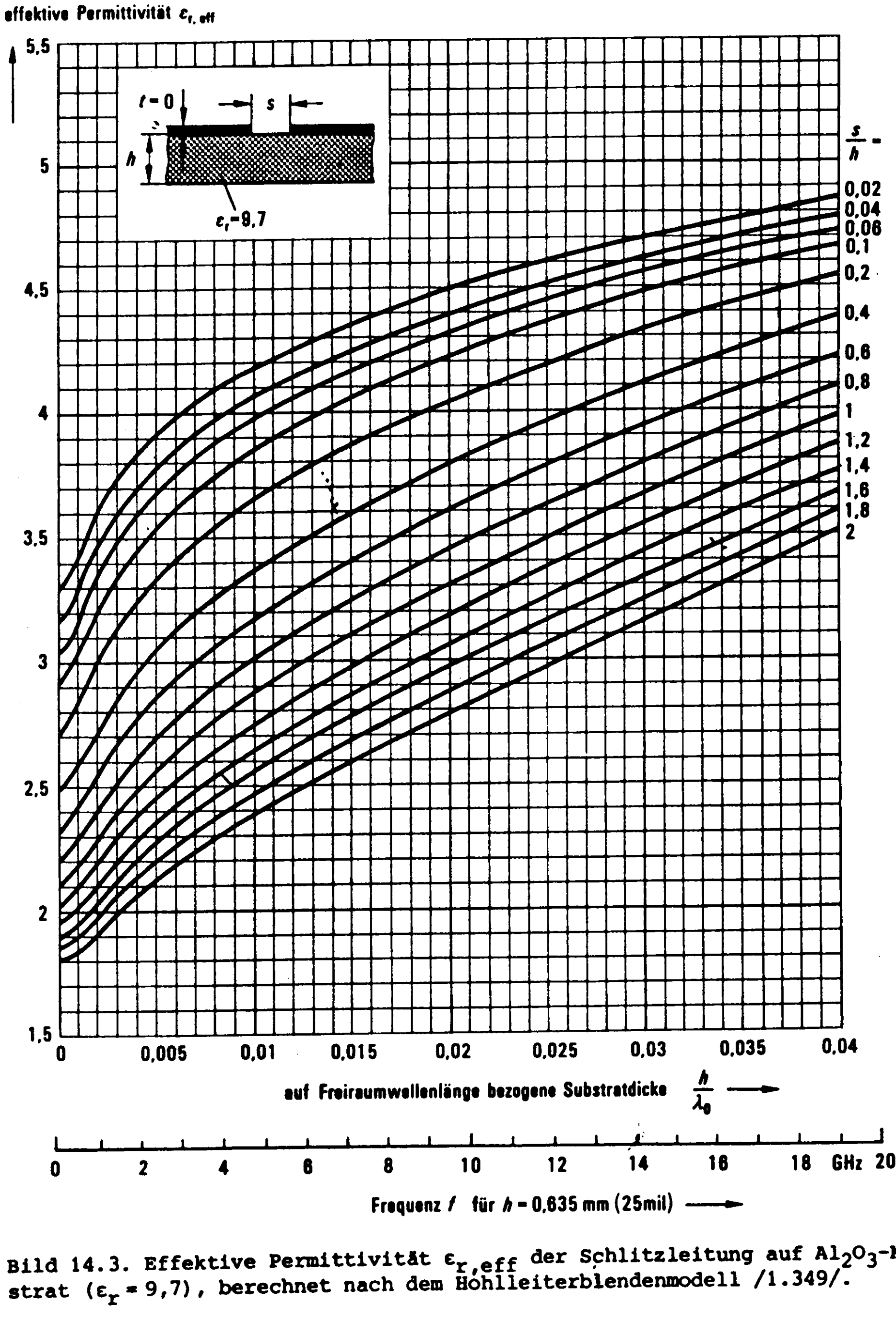

[2]

Bild 14.3. Effektive Permittivität $\varepsilon_{r,eff}$ der Schlitzleitung auf Al_2O_3-Keramiksubstrat (ε_r = 9,7), berechnet nach dem Hohlleiterblendenmodell /1.349/.

Fig 3 SLOTLINE-DISPERSION

⑤

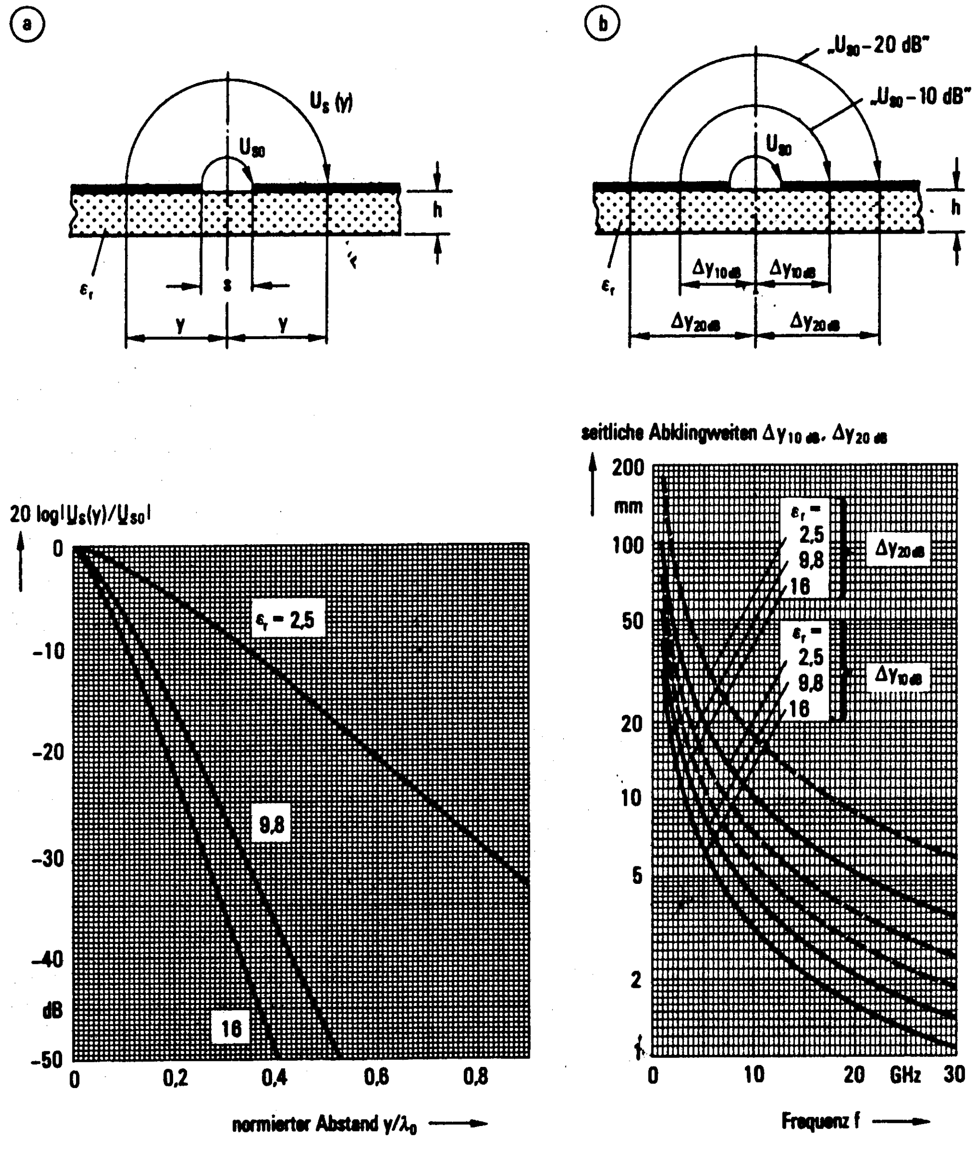

Bild 14.6. Seitliches Abklingen der Schlitzleitungsspannung in größerer Entfernung vom Schlitz. a) Seitlicher Verlauf der normierten Schlitzleitungsspannung $U_S(y)/U_{S0}$; b) seitliche Abklingweiten Δy_{10dB}, Δy_{20dB} für einen Spannungsabfall um 10 dB bzw. 20 dB

[2]

Fig 4

SLOTLINE

E-FIELD IN AIR

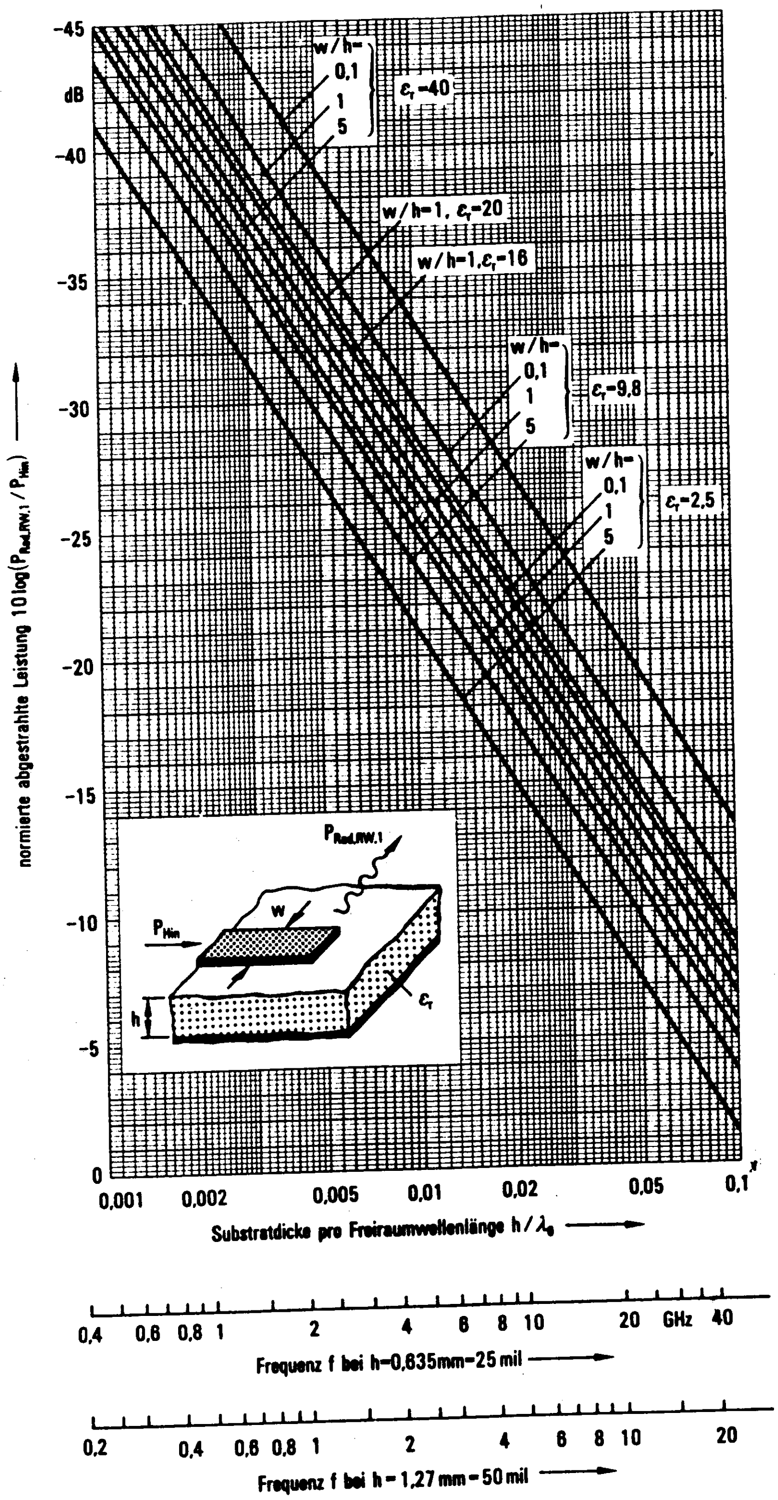

[2]

Fig 5

MICROSTRIP
OPEN END RADIATION

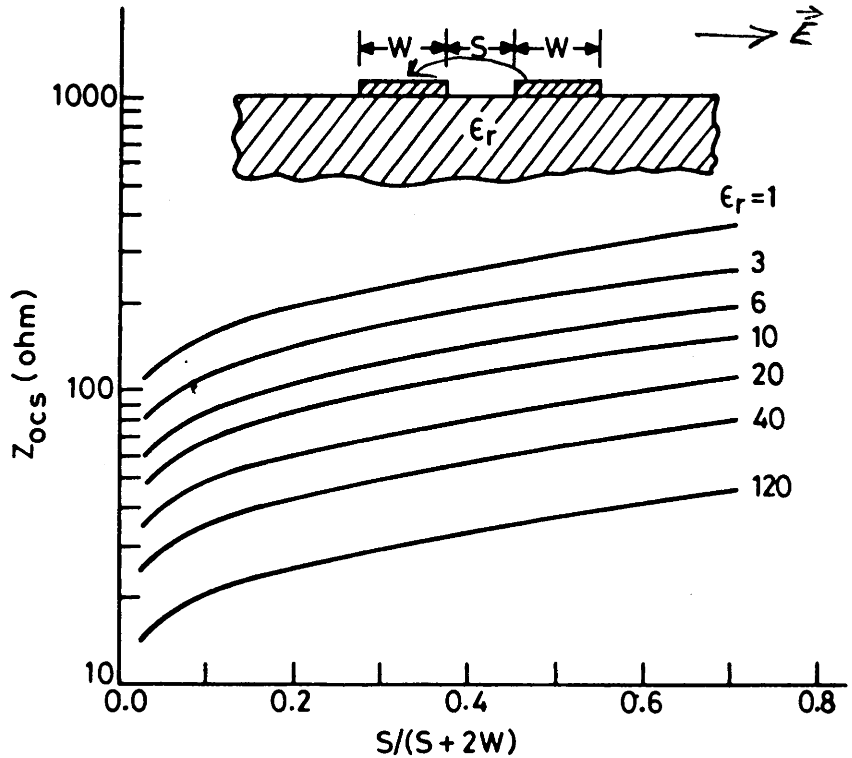

Figure 7.7 Characteristic Impedance of Coplanar Strips (from [1])

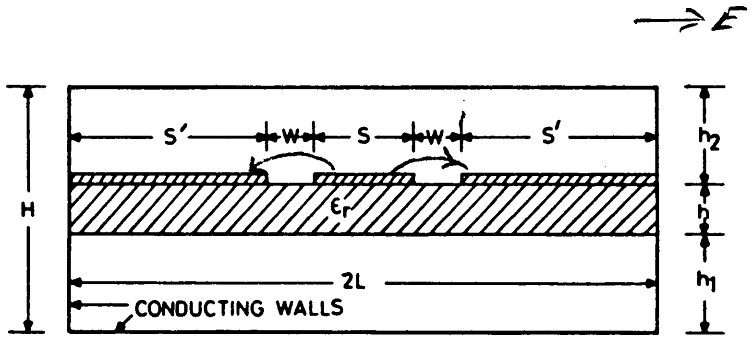

Figure 7.8 Coplanar Waveguide Enclosed in a Box

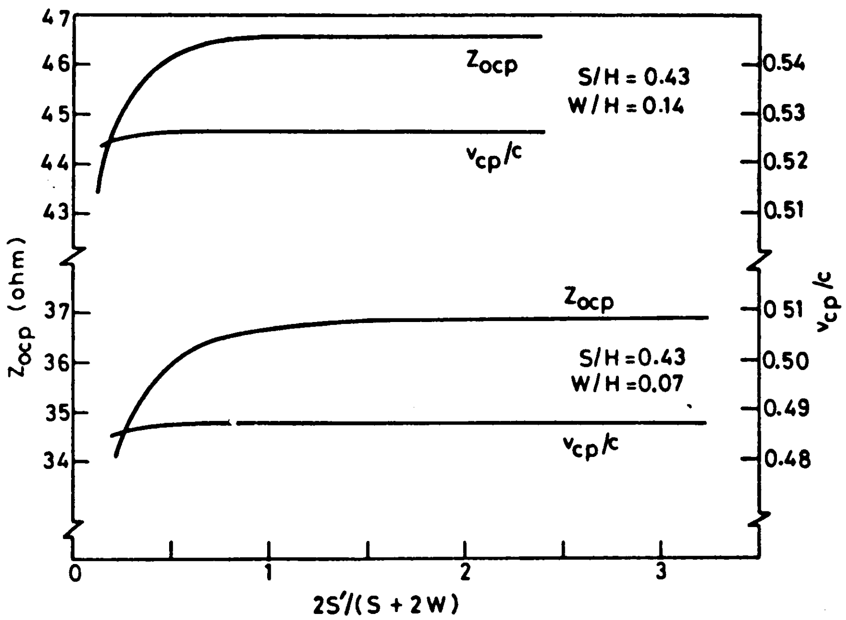

Figure 7.9 Effect of Enclosure on CPW Characteristics (from [3])

[1]

FIG 6

SPECIAL PLANAR LINES

COPLANAR STRIPS

COPLANAR WAVEGUIDE

Table 7.2 Comparison of Z_o limits
(ϵ_r = 10.0, h = 25 mil and frequency = 10 GHz)

Transmission Line	Lower limit for Z_o (ohm)	Upper limit for Z_o (ohm)
Microstrip	20 (m)	110 (d)
Slotline	55 (d)	300 (m)
Coplanar waveguide	25 (m, d)	155 (m, d)
Coplanar strips	45 (m, d)	280 (m, d)

This comparison indicates that microstrip lines are capable of providing low impedance whereas slotlines and coplanar strips may be used for very high impedances.

[1]

Table 7.3 Comparison of loss for various lines (ϵ_r = 10.0, h = 25 mil and frequency = 10 GHz)

Transmission line	Loss (dB/cm)	
	50 ohm	100 ohm
Microstrip	0.04	0.14
Slotline	0.15*	—
Coplanar waveguide (h/W=2)	0.08	0.28
Coplanar strips (h/W=2)	0.83	0.13

*ϵ_r = 16, Z_o = 75 ohm.

[1]

Table 7.5 Qualitative comparison of various MIC lines

Characteristic	Microstrip	Slotline	Coplanar waveguide	Coplanar strips
Effective dielectric constant (ϵ_r = 10 and h = 0.025 inch)	~6.5	~4.5	~5	~5
Power handling capability	High	Low	Medium	Medium
Radiation loss	Low	High	Medium	Medium
Unloaded Q	High	Low	Medium	Low (lower impedances) High (higher impedances)
Dispersion	Small	Large	Medium	Medium
Mounting of components:				
in shunt configuration	Difficult	Easy	Easy	Easy
in series configuration	Easy	Difficult	Easy	Easy
Technological difficulties	Ceramic holes Edge plating	Double side etching	—	—
Elliptically polarized magnetic field configuration	Not available	Available	Available	Available
Enclosure dimensions	Small	Large	Large	Large

[1]

FIG 7 GENERAL PROPERTIES OF MICROSTRIP, SLOTLINE, COPLANAR LINES

8

where c is the velocity of electromagnetic waves in free space. Values of characteristic impedance Z_{ocp} computed from Equation (7.6) are shown in Figure 7.4. Measured values of Z_{ocp} for $\epsilon_r = 9.6$, 16 and 130

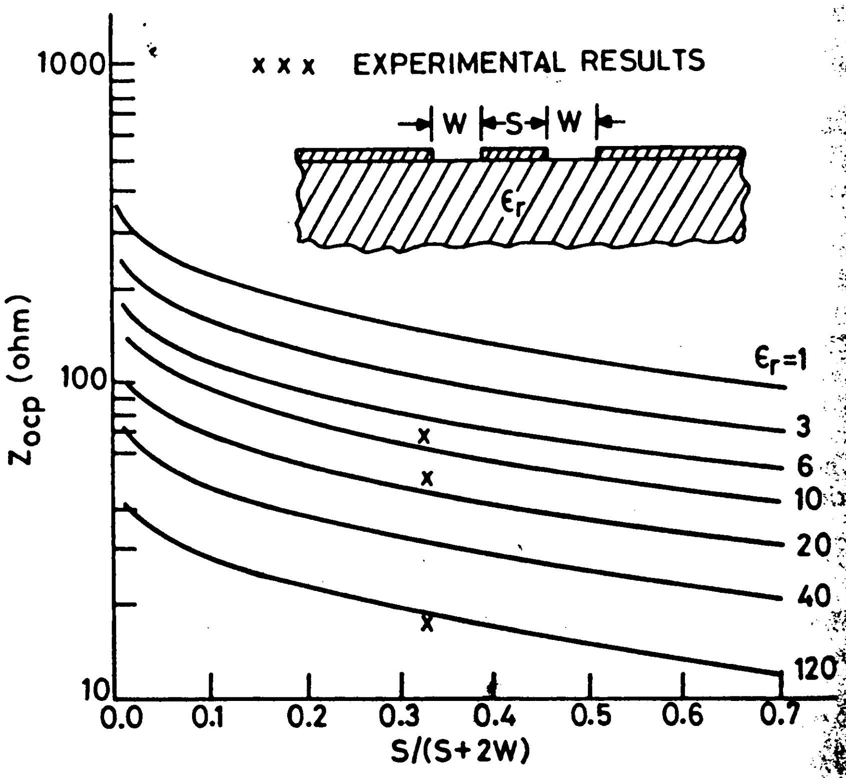

Figure 7.4 Characteristic Impedance of Coplanar Waveguides (from [1])

are also shown in this figure. Wen [1] points out that Z_{ocp} increases by less than 10 percent, for large values of ϵ_r, when the thickness of the substrate is reduced from infinite to W, the width of the slots (that is, when $W/h \rightarrow 1$).

[1]

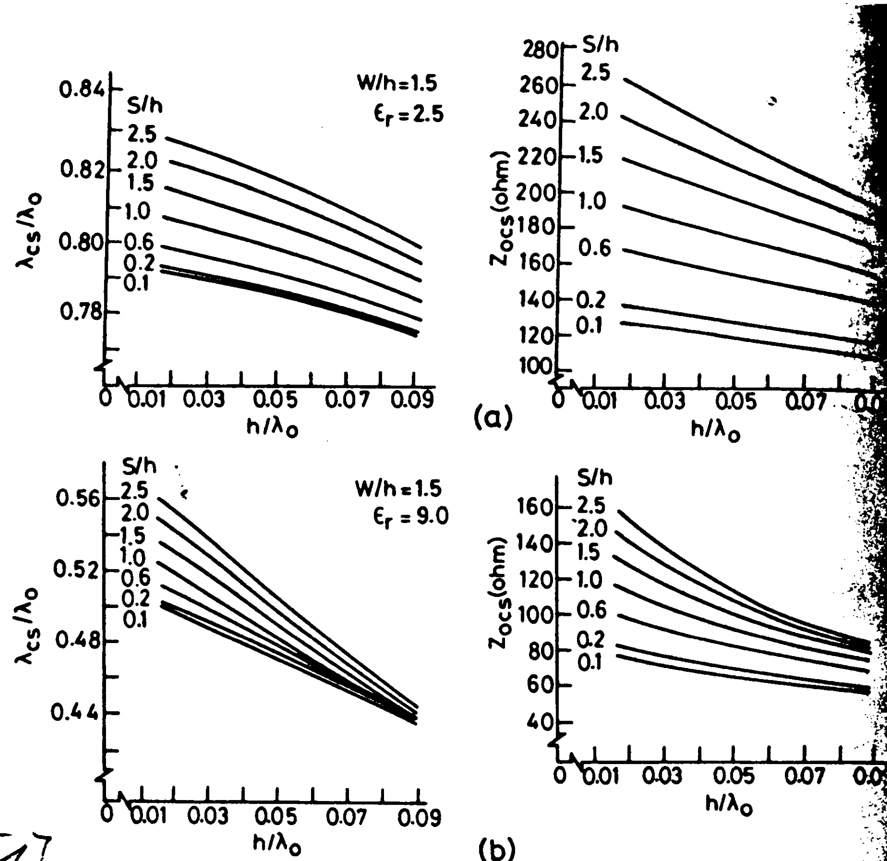

[1]

Figure 7.14 Dispersion Characteristics of Coplanar Strips (from [4])

Fig 8 IMPEDANCE OF COPLANAR LINES

9

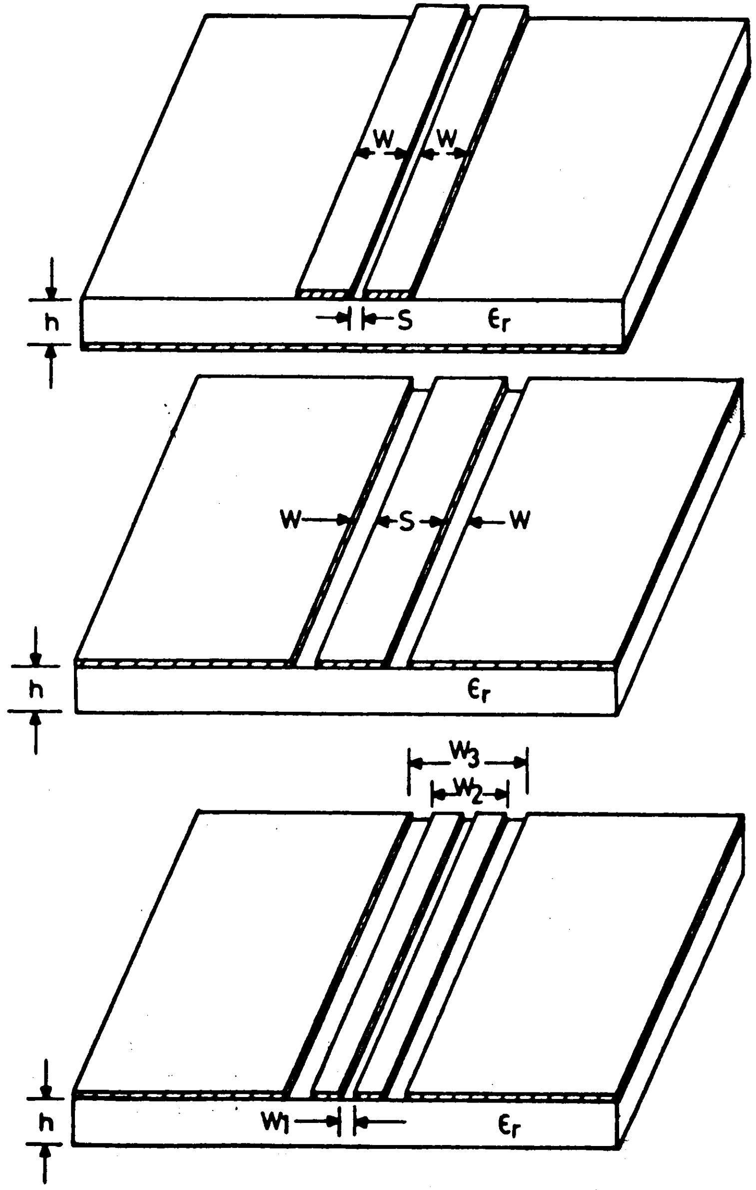

Figure 8.1 Configurations of

(a) Coupled Microstrip Lines
(b) Coupled Slotlines and
(c) Coupled Coplanar Waveguides

[1]

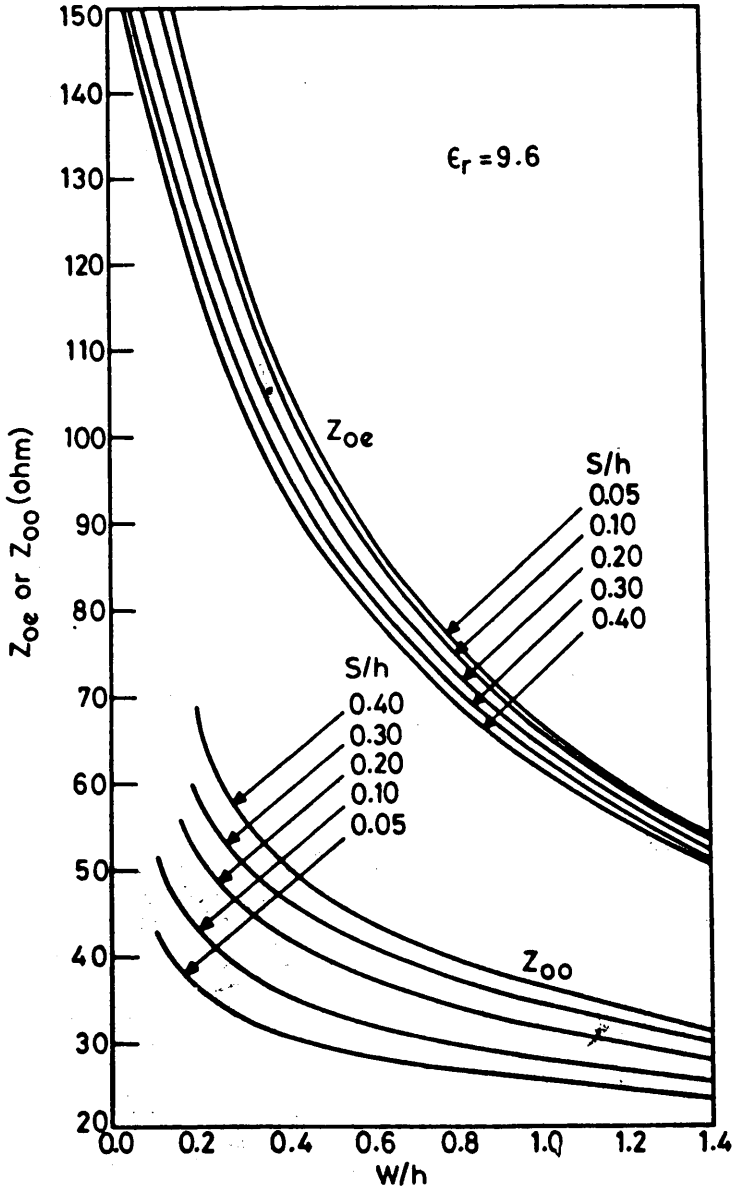

Figure 8.4(a) Even and Odd Mode Characteristic Impedances for Coupled Microstrip Lines (ϵ_r = 9.6, S/h = 0.05 to 0.4, W/h = 0.1 to 1.4) (from [18])

[1]

Fig 9 COUPLED LINES

(10)

8.6.1 Characteristics of Coupled Slotlines

Coupled slotlines are obtained by separating the two slots by a strip as illustrated in Figure 8.1(b). The width S of the strip controls the coupling coefficient. The electric field configuration for even and odd modes are shown in Figure 8.23. It may be noted that the plane of

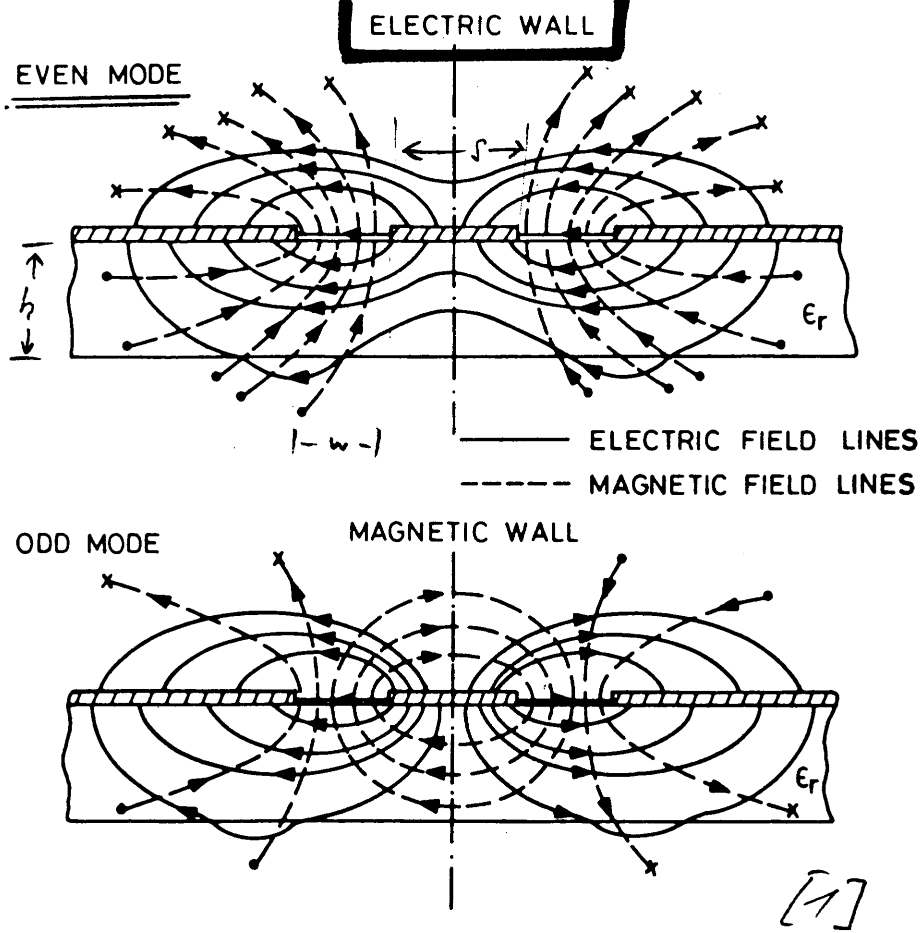

Figure 8.23 Even and Odd Mode Field Configurations in Coupled Slotlines

The characteristics of coupled slotlines are shown in Figure 8.24 for

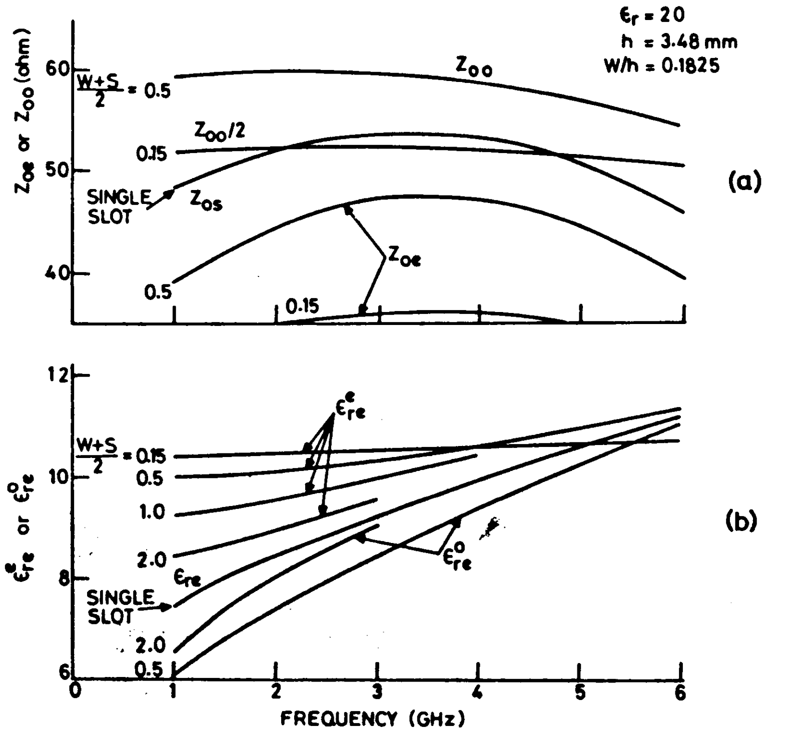

Figure 8.24 Characteristics of Coupled Slotlines, (a) Characteristic Impedance and (b) Effective Dielectric Constant (from [42])

[1]

FIG 10 COUPLED SLOTLINES (FIELDS, MODES)

11

$a_{km} = 20 \log \frac{1}{k}$

$Z_{L,even} = Z_L \sqrt{(1+k)/(1-k)}$

$Z_{L,odd} = Z_L \cdot \sqrt{(1-k)/(1+k)}$

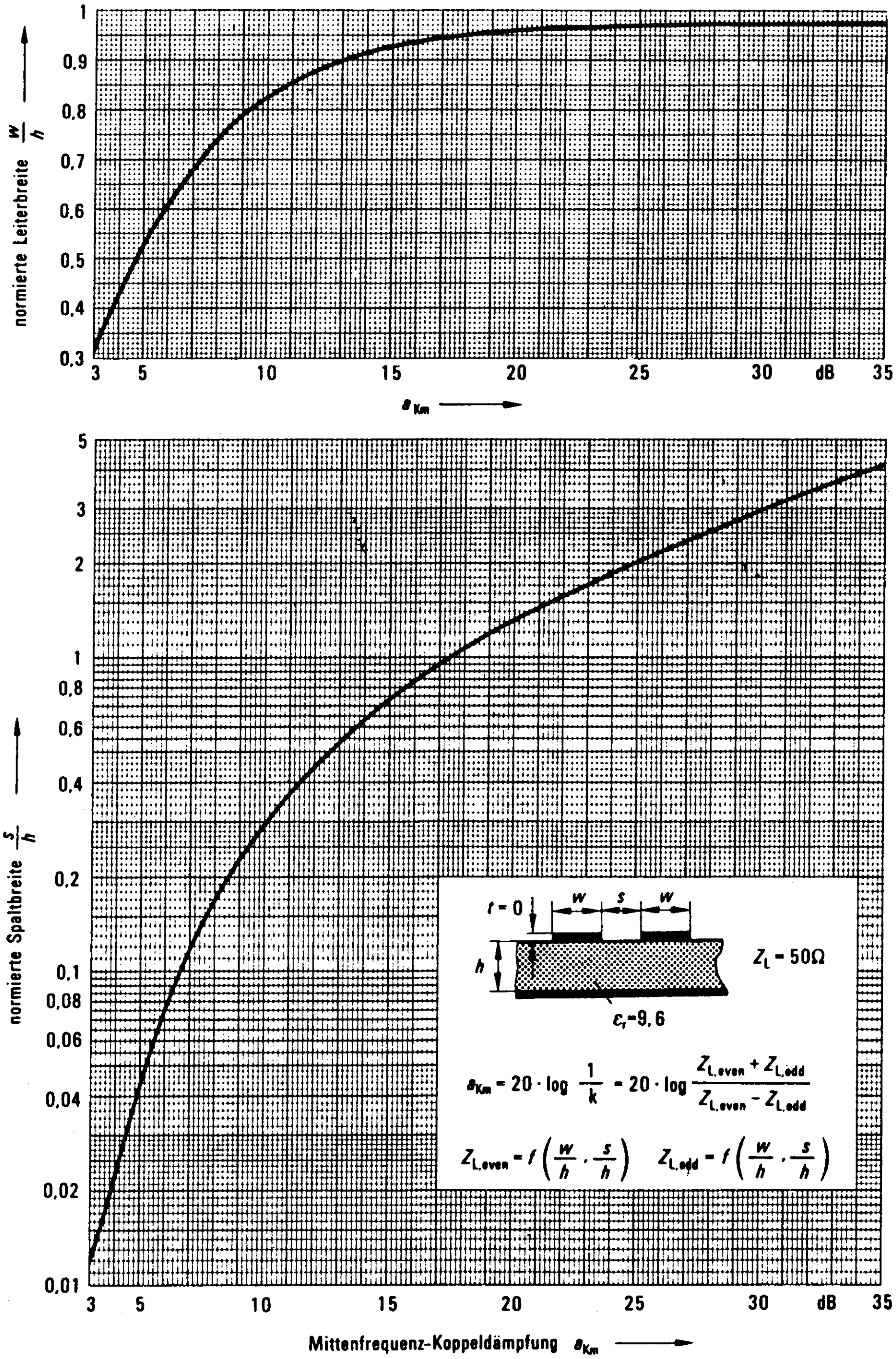

Bild 9.10. Querschnittsabmessungen w/h, s/h von Mikrostreifenleitungs-Richtkopplern für $\varepsilon_r = 9{,}6$ (Al_2O_3-Keramiksubstrat) und $Z_L = 50\,\Omega$, abhängig von der Mittenfrequenz-Koppeldämpfung a_{Km}. [2]

FIG 11 COUPLED MICROSTRIPS
DIRECTIVE COUPLERS

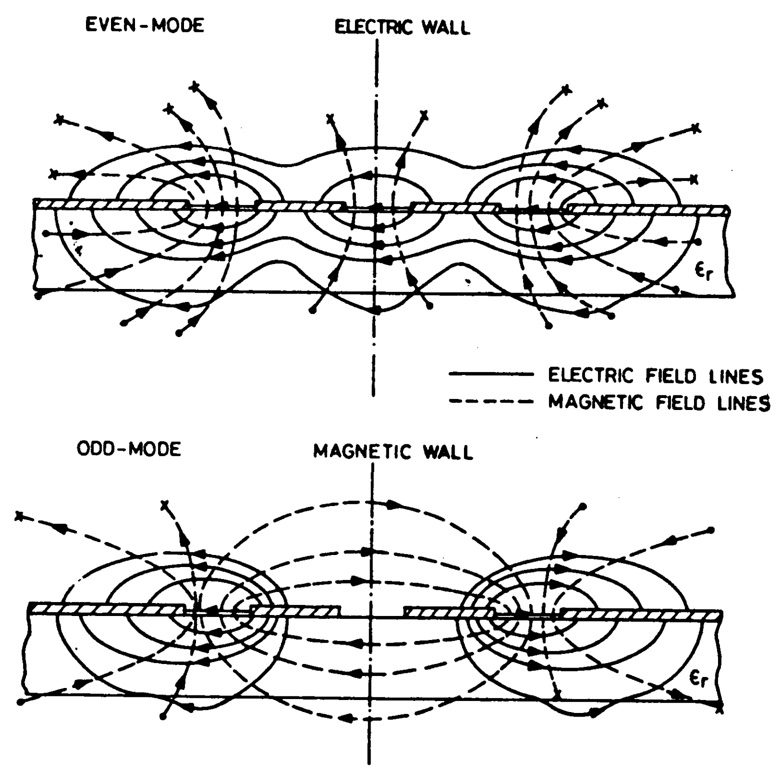

[1]

Figure 8.25 Even and Odd Mode Field Configurations in Coupled Coplanar Waveguides

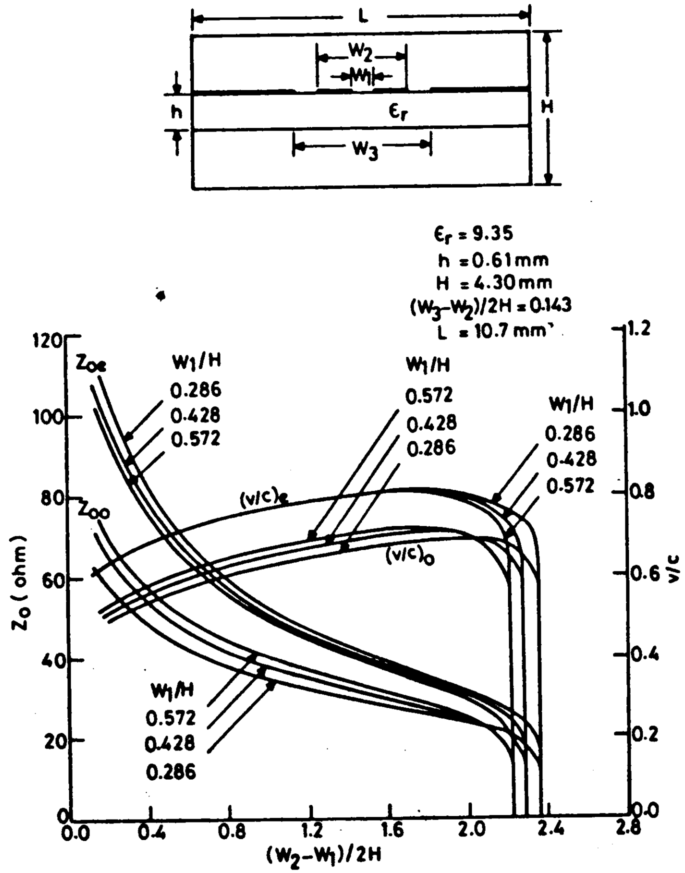

[1]

Figure 8.26 Characteristics of Coupled Coplanar Waveguides (from [44])

FIG 12 COUPLED COPLANAR LINES

13

MICROSTRIP LINES and SLOTLINES [1]

K.C. Gupta
Ramesh Garg
I.J. Bahl

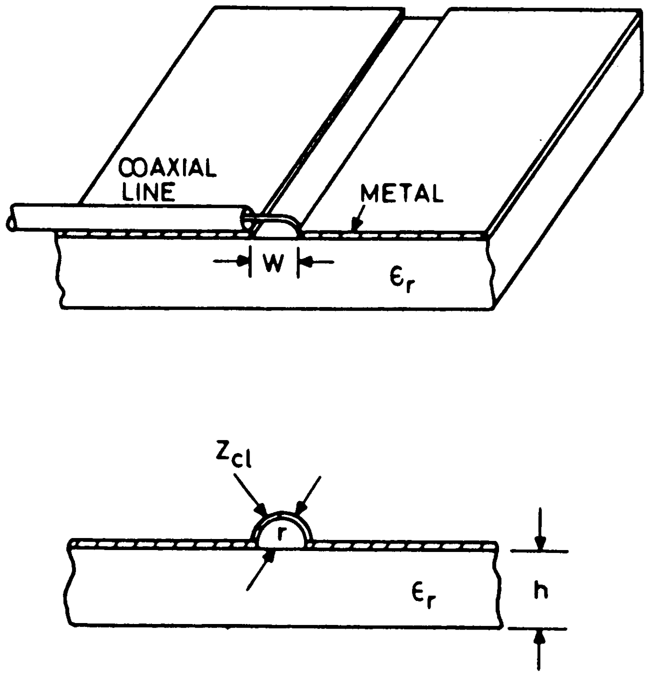

Figure 6.1 A Coaxial-to-Slotline Transition and its Model for Analysis

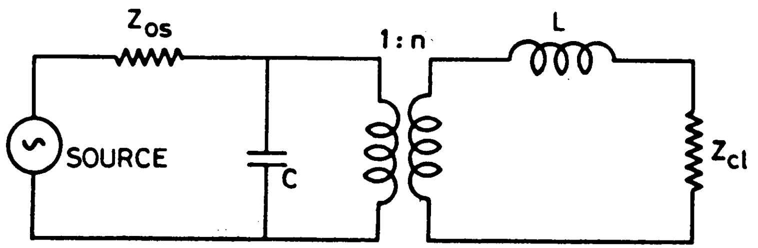

Figure 6.2 Equivalent Circuit of the Transition Shown in Figure 6.1

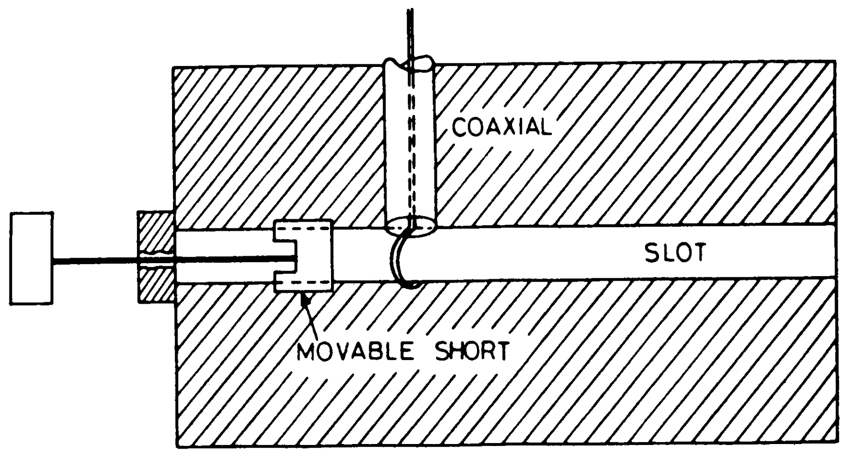

Figure 6.4 Coaxial to Slotline Transition with a Movable Short

This transition is very useful for feeding and testing slotline circuits.

FIG 12 a SLOTLINE - COAX TRANSITION

14

Microstrip to Slotline Transition Using a Cross-Junction

A microstrip-slot transition is shown in Figure 6.5(a). The slotline,

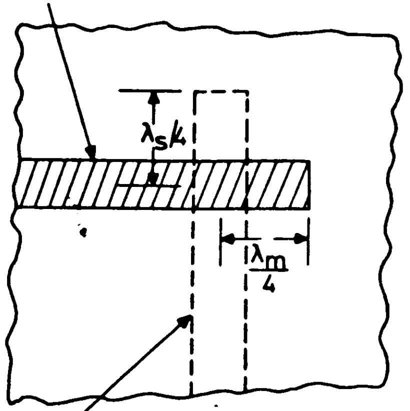

Figure 6.5(a) Microstrip-Slotline Transition

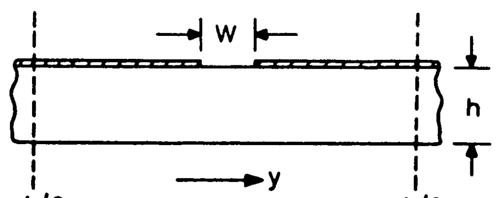

Figure 6.5(b) Slotline Cross-Section

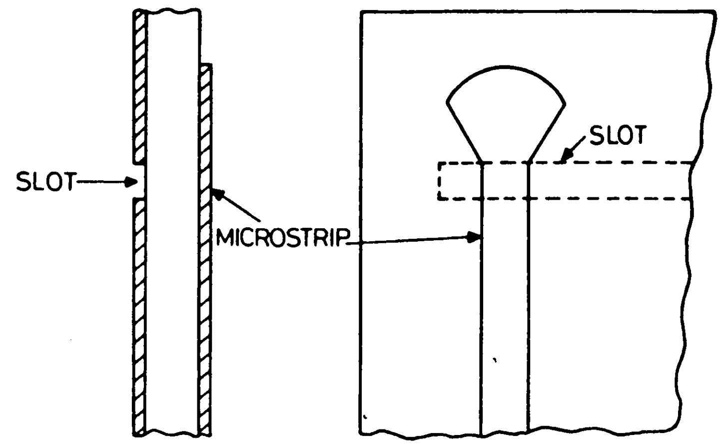

Figure 6.7 A Different Type of Microstrip-Slotline Transition

Different variations of this transition have been reported [4] for wide band applications. These are shown in Figure 6.8(a), (b) and (c). The

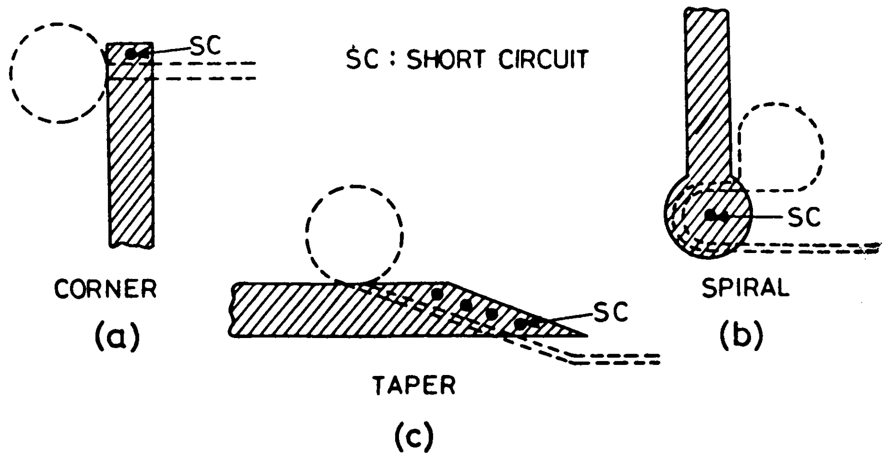

Figure 6.8 Wide Band Microstrip-Slotline Transitions

[1]

FIG 13 SLOTLINE-
MICROSTRIP TRANSITION

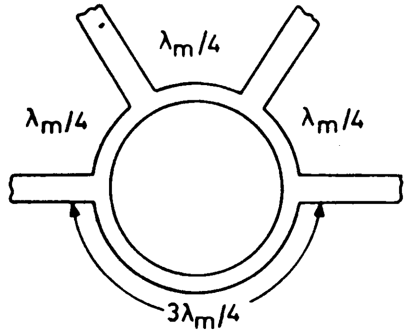

Figure 6.18(a) A Rat-Race Hybrid Using Microstrip Lines Only

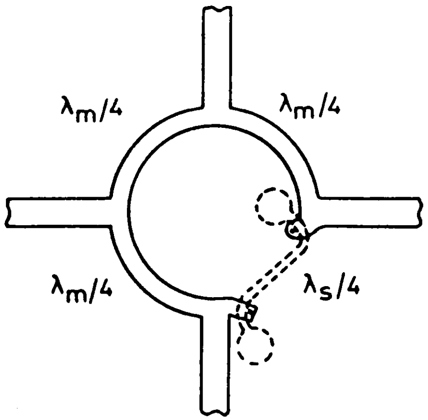

Figure 6.18(b) Rat-Race Hybrid Using Slotline in (a)

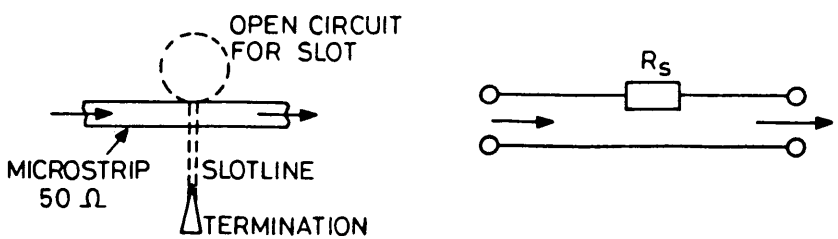

Figure 6.13(a) Microstrip-Slotline Series-T Junction and its Equivalent Circuit

6.2.2 Circuits Using Wide Band 180° Phase Shift

When two microstrip to slotline transitions are connected back-to-back as shown in Figure 6.17(a), an additional 180 degree phase

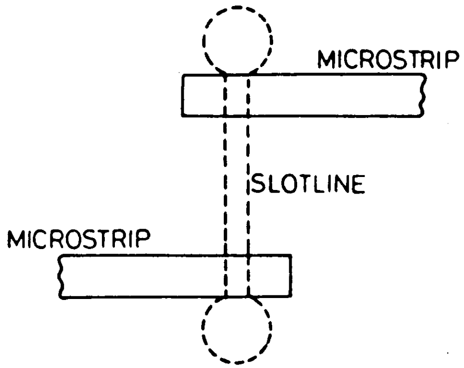

Figure 6.17(a) Two Microstrip-Slotline Transitions Connected Back-to-Back for 180° Phase Change

shift is introduced in the signal path. This can be explained qualitatively by considering the E-field distribution associated with the microstrip-slotline transition. Referring to Figure 6.17(b), we note

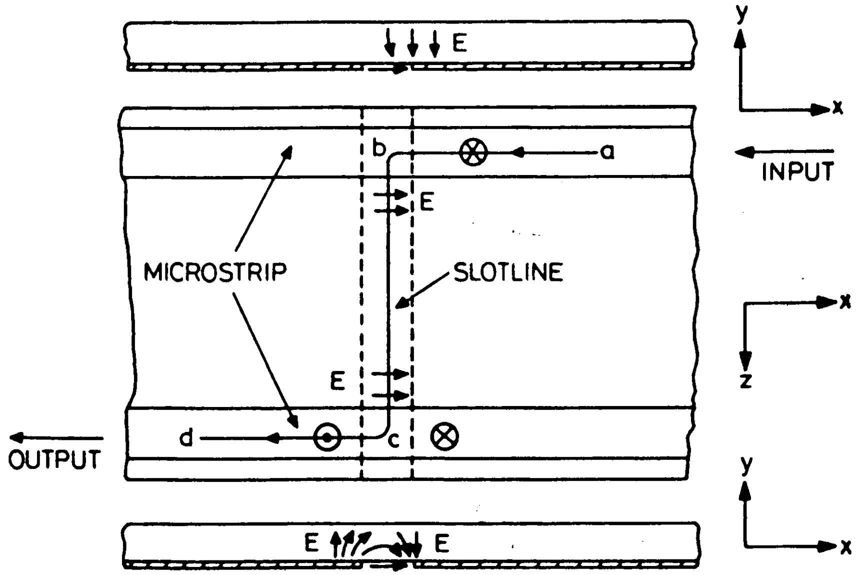

Figure 6.17(b) Mechanism for 180° Phase Change

[17]

FIG 14 SLOTLINE- MICROSTRIP TRANSITIONS